DOI:10.25092/baunfbed. 1770397 *J. BAUN Inst. Sci. Technol., 28(1), 263-273, (2026)*

Aspect ratio comparison analysis of hybrid re-entrant auxetic structures

Uğur KEMİKLİOĞLU*

Başkent University Faculty of Engineering, Department of Mechanical Engineering, Baglica Campus, Ankara.

Geliş Tarihi (Received Date): 22.08.2025
Kabul Tarihi (Accepted Date):07.11.2025

Abstract

In this study, sixteen models are designed with reentrant honeycomb geometry with different angles. Using the finite element method (FEM), a displacement on the horizontal axis is applied to the designed models and the vertical displacement values resulting from the applied horizontal displacement are determined and compared. Accordingly, with a horizontal displacement of 2 mm, the ratio of vertical strain to horizontal strain is found to be 2.51%, which is the highest, and 2.01%, which is the lowest. It is observed that the equivalent stresses increase with increasing angles in the design.

Keywords: *Metamaterials, geometrical design, auxetics, flexibility, finite element method.*

Hibrit girintili ökzetik yapıların en-boy oranı karşılaştırma analizi

Öz

Bu çalışmada, farklı açılara sahip girintili ökzetik geometrisine sahip on altı model tasarlanmıştır. Sonlu elemanlar yöntemi kullanılarak, tasarlanan modellere yatay eksende 2 mm yer değiştirme uygulanmış ve uygulanan yatay yer değiştirmeden kaynaklanan düşey yer değiştirme değerleri belirlenerek karşılaştırılmıştır. Buna göre, 2 mm yatay yer değiştirmede, düşey gerinim/yatay gerinim oranı en yüksek %2.51, en düşük %2.01 olarak bulunmuştur. Ayrıca, modelde oluşan karşılaştırmalı gerilmelerin, tasarımdaki artan açılarla birlikte arttığı da gözlemlenmiştir.

Anahtar kelimeler: *Meta-malzemeler, geometrik tasarım, ökzetikler, esneklik, sonlu eleman metodu.*

* Uğur KEMİKLİOĞLU, ukemiklioglu@baskent.edu.tr, http://orcid.org/0000-0002-5597-1256

1. Introduction

Auxetic structures have extremely superior engineering properties compared to structures made of traditional materials. The most important of these superior properties is that as the length increases, the cross-section widens, as the length decreases, the cross-section narrows. Much research has focused on auxetic structures, i.e. cellular structures with a negative Poisson's ratio. The ratio of longitudinal strain to transverse strain under an applied load is called Poisson's ratio. In most cases, a structure with a positive Poisson's ratio shrinks in the transverse loading direction and expands in the tensile loading direction. Conversely, the structure is considered auxetic or with a negative Poisson's ratio if it expands laterally instead of contracting. When comparing auxetic materials with negative Poisson's ratio to conventional materials with positive Poisson's ratio, it exhibits various mechanical properties such as: improved fracture toughness, increased transverse shear modulus, resistance to in-plane indentation, high wear resistance, dynamic qualities including high impact resistance and shaft damping performance [1-3]. In order to examine the shape changes and stresses in auxetic structures, compressive forces [4] and bending moments [5] are applied numerically; upon examining the free vibration analysis [6,7] and acoustic behavior [8], various mechanical analyzes are also applied numerically and the results are discussed. Along with the numerical studies applied to auxetic structures, experimental studies are also carried out and the results obtained are presented comparatively, in a good agreement [9-13]. Sahu et al. [12] investigated the energy absorption properties of these structures numerically and experimentally depending on the change of cell parameters in the auxetic structure by using honeycomb sandwich structures fabricated with two different thermoplastic elastomers. It has been confirmed both experimentally and numerically that nylon honeycomb cores with cell size diversity have better energy absorption properties. At the same time, experimental results indicate that the hardness effect also gives positive results. In another study by Valle et al. [14], the orthotropic behavior of Auxetic structures was compared experimentally to analytical solutions using Timoshenko beam theory.

The mechanical properties exhibited by auxetic structures; their physical behavior is also investigated. For instance, Shan et al. [15] have developed different structures for architectural materials that can absorb elastic energy and fully close under the influence of compressive forces. They examined the tendency for the change in the cross-section to be completely closed during the displacement applied in the direction of compression. Also, it is seen that various applications and research have been carried out on the self-folding of complex origami-inspired structures from flat shapes [16-19]. In another study, Wang et al. [20] examined the deformations occurring in axial and rotational directions based on the fishbone model. They explained the formation of polarity through various numerical and experimental studies they performed on the model they created with hard and soft surfaces.

In addition to the different geometries used to create auxetic structures, such structures have been created using sinusoidal curves and various studies have been carried out on these structures numerically [21-23]. Liu et al. [22] investigated the relationship between the change in Poisson's ratio and stiffness ratio of auxetic structures created using sinusoidal curves. They emphasized that for such two-dimensional auxetic structures, Poisson's ratio can be designed with an adjustable feature.

Studies are also being carried out to use auxetic structures in a certain area. Li et al. [24] have conducted research on the creation of force sensors using re-entrant auxetic structure. They emphasized that the structure they created could be a force sensor by using re-entrant auxetic structure as a spring.

When all the studies on auxetic structures are examined, it is noticeable that various studies have been carried out to determine the different physical and mechanical properties of the elements with this structure, since their perpendicular directions show increasing or decreasing behavior in the same direction. Gibson et al [25] carried out analytical research on the mechanical characteristics of a reentrant structure and validated their findings through experiments. The authors created models to depict the bending, elastic buckling, and plastic collapse mechanical characteristics of the structure, through the reentrant model they designed, shown in Figure 1, they obtained an equation regarding Poisson's ratio.

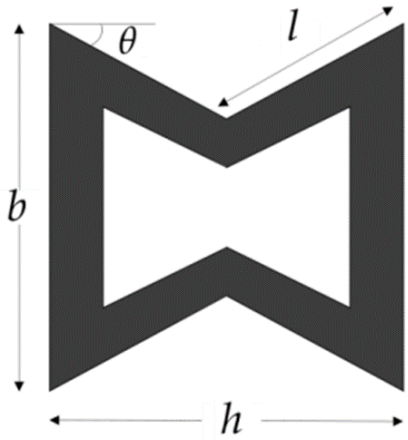

Figure 1. Re-entrant model dimensions.

In this model, h represents the horizontal length, b represents the height, and l represents the oblique length, and θ represents the angle value of the auxetic structure with the horizontal. Poisson's ratio was calculated with the equation below, and it was stated that it depends on the θ, b and l measurements in the model.

$$\vartheta_{12} = -\frac{\sin(\theta)}{\sin(\theta)+\frac{b}{l}} \tag{1}$$

In this study, it is aimed to examine only the effect of angular change on Poisson's ratio, regardless of the lengths b and l: For this reason, the lengths in the structure are designed to be equal. Within the scope of this study, 8 re-entrant auxetic geometries are combined with each other to create an auxetic structure with an axis of symmetry. The internal angles of this structure, which is created from beam elements of the same length, are defined as 70°, 75°, 80° and 85° degrees and accordingly, it is aimed to find the maximum vertical displacement value that could occur as a result of the horizontal displacement applied to such structures. Within the results obtained; the ideally determined structure can be used as the tension mechanism of a machine part or in the design of a trampoline mechanism that will provide maximum surface area with tensile force and in such application areas.

2. Geometrical design

In the geometric design, a re-entrant auxetic honeycomb model with the same side lengths is created to compare the extent of deformation at different angles. SolidWorks (MA, USA) software is used in design. The length of each beam element used in the re-entrant honeycomb geometry is 500 mm, and the angles forming the geometry vary as 70, 75, 80 and 85 degrees. The sketch of re-entrant geometry, with the horizontal (x) and vertical (y) directions, where the angle is defined as α is shown in Figure 2.

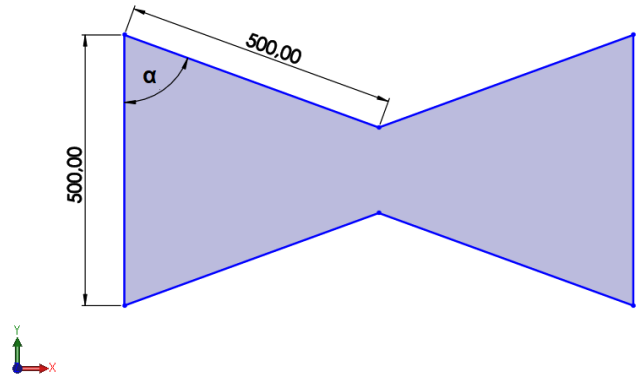

Figure 2. The sketch of re-entrant auxetic geometry.

Once the two dimensional (2D) model sketch has been designed in Solidworks, the final profile is drawn. When creating the reentrant honeycomb model in which the displacements are to be investigated, 8 auxetic honeycomb geometries are arranged symmetrically. The internal angles used in the creation of the re-entrant auxetic models are shown as α and β in Figure 3. The cross-sectional length of the re-entrant honeycomb model is 40x40 mm^2. Since α and β angles are positioned as 90°-θ in the hybrid model shown in Figure 3, Equation 1 has been revised as follows.

$$\vartheta_{xy} = -\frac{\cos(\alpha)}{\cos(\alpha)+1} \tag{2}$$

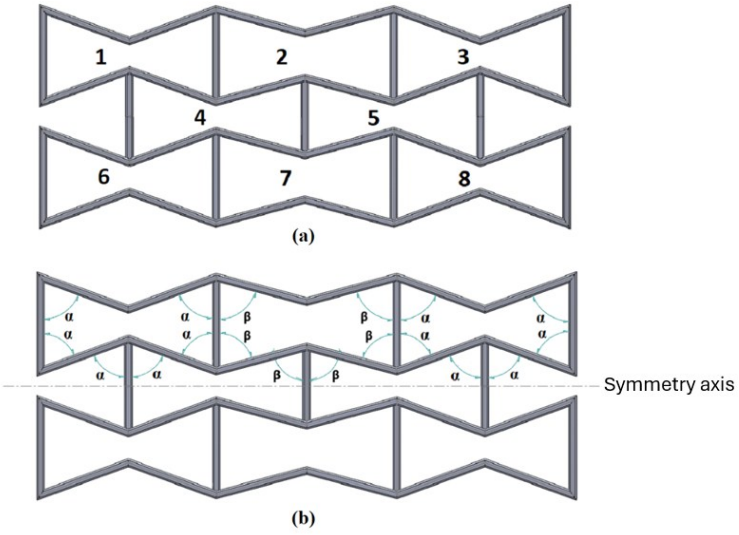

Figure 3. Re-entrant auxetic model: a) 8 set auxetic geometries, b) varying angles as α and β.

Totally 8 set auxetic geometries numbered from 1 to 8 can be seen in Figure 3(a). The α and β interior angles are seen in Figure 3(b). Geometry 4 and 5 are positioned with α and β interior angles at the middle of the model, while geometry 1, 3, 6, 8 are positioned with α interior angles at the corners of the model, and geometry 2 and 7 are positioned with β interior angles.

In these models, auxetic geometries with α (alpha) interior angles are called geometry A; and auxetic geometries with β (beta) interior angles are called geometry B. Auxetic geometries with both angles (4^{th} and 5^{th} geometries in Figure 3a) are defined as hybrid geometry. Geometry A, geometry B and hybrid geometry of the auxetic model is shown in Figure 4 with yellow (A) and blue (B) colors.

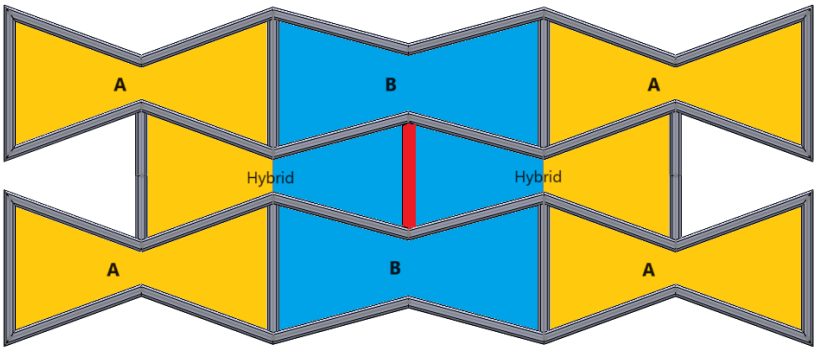

Figure 4. Auxetic model consisting of A, B and hybrid geometries.

As seen in Figure 4, the length of the gray beam elements remains constant (500 mm), the length of the red beam element located in the geometric center of the model varies as the angles change. The red beam element is defined as center beam element.

Parametrically; 16 different models have been designed in which the interior angles vary between 70, 75, 80, 85 degrees, respectively. The 16 parameters are shown in Table 1, with their named form.

Table 1. Model names with geometric angles.

M(α;β)	**1.** β=70°	**2.** β=75°	**3.** β=80°	**4.** β=85°
1. α=70°	M11	M12	M13	M14
2. α=75°	M21	M22	M23	M24
3. α=80°	M31	M32	M33	M34
4. α=85°	M41	M42	M43	M44

As can be seen from Table 1; M11, M22, M33 and M44 models are homogeneous auxetic models created with angles of 70, 75, 80 and 85 degrees, respectively.

A constant value of displacement on the horizontal axis (x) was applied to 16 auxetic models created with different interior angles using the finite element method (FEM), and the displacement values of these models on the vertical axis (y) were compared from largest to smallest.

3. FEM Analysis of auxetic models

Static structural analysis is applied to the auxetic models via ANSYS software (PA, USA). The auxetic model is fixed on one side along its vertical axis, and 2 mm displacement is applied in the horizontal direction on the other side. Thereby, boundary conditions are determined as shown in Figure 5. The material type used in the analyzes is defined as structural steel.

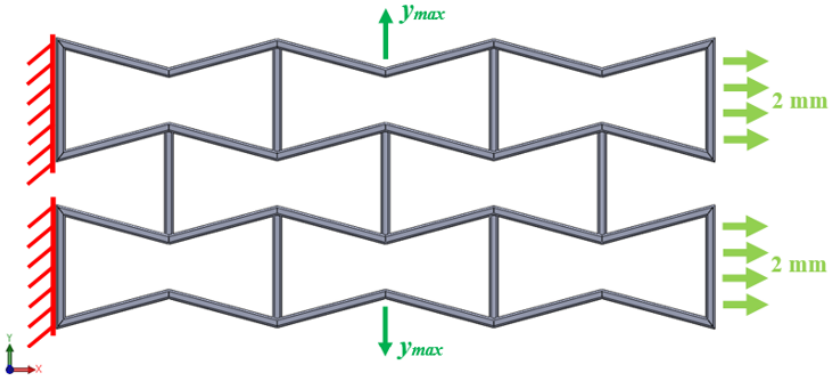

Figure 5. Boundary conditions of structural analysis.

The meshes needed for separation into finite elements are generated as 0.5 mm element size. As a result of the analyses, the maximum values of vertical displacements on y direction of each model are calculated. Along with the analyses, the length of center beam element is also determined, and comparisons are made between maximum vertical displacement values due to the center beam length change. The length values of the center beam element measured from all models are given in Table 2.

Table 2. Length of center beam elements (mm).

M(α;β)	**β=70°**	**β=75°**	**β=80°**	**β=85°**
α=70°	**500**	417	332	245
α=75°	583	**500**	415	328
α=80°	668	585	**500**	414
α=85°	755	672	587	**500**

The M41 model has a maximum length of 755 mm, while the M14 model has a minimum length of 245 mm. The difference between these two models is; While the alpha angle of the M41 model is the maximum value of 85°, the beta angle is the minimum value of 70°. For the M14 model, the alpha and beta angles are vice versa. Angle values between 70° and 85°, from minimum to maximum, are determined in the designed models, considering the preservation of the auxetic form.

4. Results and discussions

The vertical deformations and equivalent stress values of the auxetic models because of 2 mm displacement applied in the horizontal direction are examined using the finite element method. Therewithal, the horizontal and vertical lengths of the auxetic models

before deformation, given in Table 3, are measured, and the relationships between these lengths and the vertical displacement after deformation were also investigated.

Table 3. Width and height of auxetic models.

M(α;β)	Width (mm)				Height (mm)
	β=70°	β=75°	β=80°	β=85°	For all β angles
α=70°	2839	2885	2904	2916	1215
α=75°	2912	2937	2957	2968	1293
α=80°	2949	2976	2994	3006	1374
α=85°	2972	2998	3017	3029	1457

While the beta angle is constant, horizontal, and vertical lengths increase as the alpha angle increases, as seen in Table 3. It is seen that width of the auxetic model also increases as the alpha and beta angles increase as seen in Figure 6(a). Although the heights of all beta angle models with the same alpha angle are the same, the height of the auxetic model increases as the value of the alpha angle increases as seen in Figure 6(b).

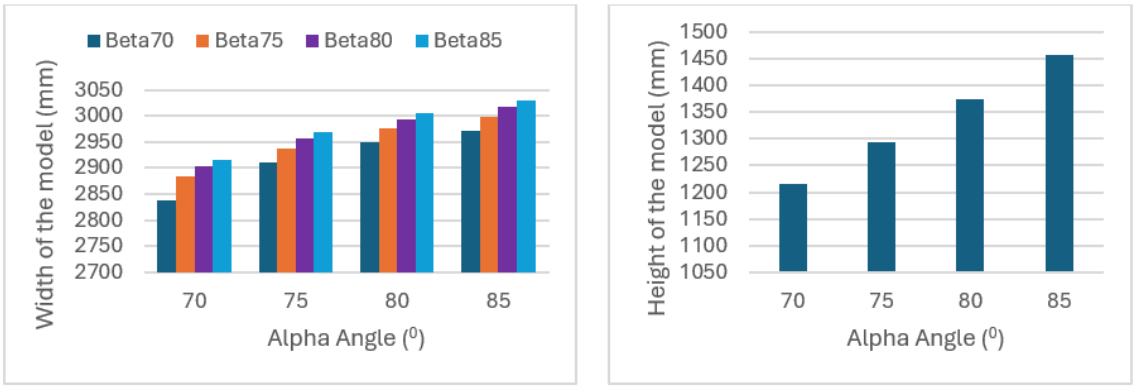

(a) **(b)**

Figure 6. Auxetic model lengths: a) Length of width, b) Length of height.

According to the block diagrams shown in Figure 5, increasing the alpha and beta angles causes the volume of the model to increase.

Vertical displacement (Y_{max}) values resulting from 2 mm horizontal displacement applied to all models and maximum equivalent stress (σ_{eq}) values occurring on the model are given in Table 4.

Table 4. Vertical displacement and maximum equivalent stress values of auxetic models.

M(α;β)	Y_{max} *(mm)*				σ_{eq} *(MPa)*			
	β=70°	β=75°	β=80°	β=85°	β=70°	β=75°	β=80°	β=85°
α=70°	2.2116	2.1249	**2.0239**	2.2147	**231**	262	291	320
α=75°	2.8234	2.8146	2.5143	2.6326	287	271	323	373
α=80°	3.5862	3.7761	3.5611	3.0376	367	347	384	461
α=85°	4.1726	4.8338	**5.0220**	3.7898	405	458	407	**569**

When the vertical displacements are examined according to Table 5, it is seen that the M13 model has the minimum displacement, while the M43 model has the maximum displacement. The minimum and maximum vertical displacement images obtained from the 2 mm horizontal displacement applied to the models are shown in Figure 7.

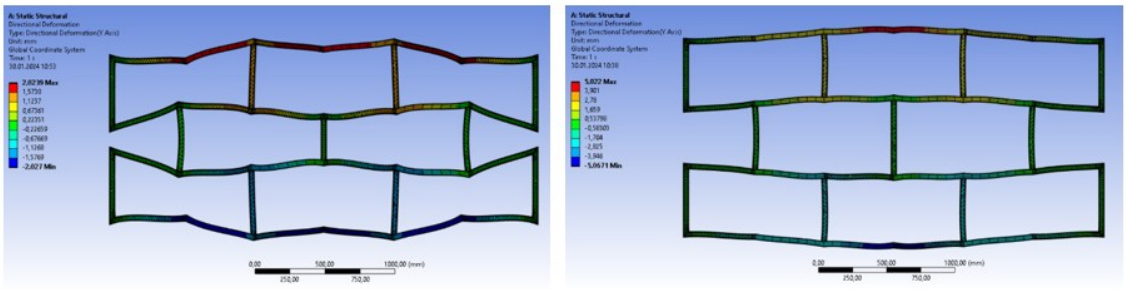

(a) **(b)**

Figure 7. FEM images of vertical displacements; a) Minimum displacement of model M13, b) Maximum displacement of model M43.

It is seen that the displacement has minimum and maximum values when the beta angle is 80°. Furthermore, while the beta angle is constant for all models, the vertical displacement values increase as the alpha angle increases.

When the equivalent stresses occurring because of horizontal displacement applied to the models are examined, it is seen that as the alpha and beta angles increase from 70° to 85°, respectively; the maximum equivalent stress in the models also increases. Images of the M11 and M44 models, from which the minimum and maximum equivalent stresses are obtained from Ansys, are given in Figure 8.

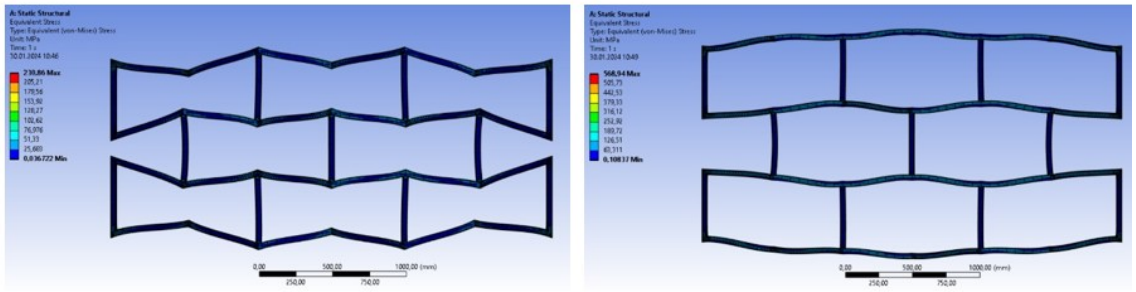

(a) **(b)**

Figure 8. FEM images of maximum equivalent stress; a) M11 model, b) M44 model.

It is seen that stress and displacement values are obtained regardless of the width and height of the auxetic models. In addition, the minimum or maximum length of the center beam element cannot be associated with the stress and displacement values. It can be mentioned that maximum and minimum stress and displacement values are obtained depending on the changing angle.

5. Conclusion

A model is created using auxetic geometries created at different angles from square-section profiles of the same length. The vertical displacement values resulting from the

2 mm horizontal displacement applied to these models with different angles and the maximum equivalent stresses occurring in the models are obtained and examined by the FEM. Afterwards the design and analysis, the following results were obtained:

The total width of the models created by combining 8 auxetic geometries at different angles varies. This width value increases as the alpha angle increases while the beta angle is constant. As well as the Beta angle increases, the total width also increases. The total height of the auxetic model increases only with increasing alpha angle. Beta angle has no effect on the total height.

Vertical displacements resulting from the 2 mm horizontal displacement applied to auxetic models produce different results depending on different angles: The maximum vertical displacement against horizontal displacement is 5.022 mm in the M43 model (α 85°; β 80°), which is 151% more than the horizontal displacement value. The minimum vertical displacement is 2.0239 mm in the M13 model (α 70°; β 80°) and this value is almost close to the horizontal displacement value. As the alpha and beta angles increase, the stress values on the model also increase.

Consequently, for this model consisting of 8 auxetic geometries, the beta angle of 80° causes maximum and minimum displacements.

References

[1] Wu W, Hu W, Qian G, Liao H, Xu X, and Berto F. Mechanical design and multifunctional applications of chiral mechanical metamaterials: A review. **Materials and Design** 2019; 180. Doi: 10. 1016/j. matdes. 2019. 107950

[2] Ren X, Das R, Tran P, Ngo TD, and Xie YM. Auxetic metamaterials and structures: a review. **Smart Mater Struct** 2018; 27(2):023001. Doi: 10. 1088/1361-665X/aaa61c

[3] Novak N, Vesenjak M, and Ren Z. Auxetic Cellular Materials – a Review. **Strojniški vestnik - Journal of Mechanical Engineering** 2016; 62(9), 485-493. Doi: 10. 5545/sv-jme. 2016. 3656

[4] Shruti M, Hemanth NS, Badgayan ND, and Sahu SK. Compressive behavior of auxetic structural metamaterial for lightweight construction using ANSYS static structural analysis. **Materials Today: Proceedings** 2021; 38, 12-17. Doi: 10. 1016/j. matpr. 2020. 05. 410

[5] Dutta S, Menon HG, Hariprasad MP, Krishnan A, and Shankar B. Study of auxetic beams under bending: A finite element approach. **Materials Today: Proceedings** 2021; 46, 9782-87. Doi: 10. 1016/j. matpr. 2020. 10. 479

[6] Kushwaha YS, Hemanth NS, Badgayan ND, Sahu SK. Free vibration analysis of PLA based auxetic metamaterial structural composite using finite element analysis. **Materials Today: Proceedings** 2022; 56, 1063-67. Doi: 10. 1016/j. matpr. 2021. 09. 482

[7] Kemiklioğlu U. Novel Design and Comparison of Structural and Modal Analyses of Auxetic Geometry versus Honeycomb Geometry. **International Polymer Processing** 2021; 36. Doi: 10. 1515/ipp-2020-4067

[8] Meaud J, and Che K. Tuning elastic wave propagation in multistable architected materials. **International Journal of Solids and Structures** 2017; 122, 69-80. Doi: 10. 1016/j. ijsolstr. 2017. 05. 042

[9] Ma X, Zhang N, Zhang C, and Tian X. Mechanical behavior of a novel lattice structure with two-step deformation. **Thin-Walled Structures** 2024; 197:111580. Doi: 10. 1016/j. tws. 2024. 111580

[10] Ha CS, Lakes RS, and Plesha ME. Cubic negative stiffness lattice structure for energy absorption: Numerical and experimental studies. **International Journal of Solids and Structures** 2019; 178-179, 127-35. Doi: 10. 1016/j. ijsolstr. 2019. 06. 024

[11] Khan SZ, Masood SH, and Cottam R. Mechanical properties in tensile loading of H13 re-entrant honeycomb auxetic structure manufactured by direct metal deposition. **MATEC Web Conferences** 2015; 34. Doi: 10. 1051/matecconf/20153401004

[12] Sahu SK, Badgayan ND, Samanta S, and Sreekanth PSR. Evaluation of Cell Parameter Variation on Energy Absorption Characteristic of Thermoplastic Honeycomb Sandwich Structure. **Arabian Journal for Science and Engineering** 2021; 46, 12487–12507. Doi: 10. 1007/s13369-021-05987-9

[13] Correra DM, Klatt T, Cortes S, Haberman M, Kovar D, and Seepersad C. Negative stiffness honeycombs for recoverable shock isolation. **Rapid Prototyping Journal** 2015; 21(2), 193-200. Doi: 10. 1108/RPJ-12-2014-0182

[14] Valle R, Pincheira G, Tuninetti V, Garrido C, and Treviño C. Evaluation of the Orthotropic Behavior in an Auxetic Structure Based on a Novel Design Parameter of a Square Cell with Re-Entrant Struts. **Polymers** 2022; 14, 4325. Doi: 10. 3390/polym14204325

[15] Shan S, Kang SH, Raney JR, Wang P, Fang L, Candido F, Lewis JA, and Bertoldi K. Multistable Architected Materials for Trapping Elastic Strain Energy. **Adv. Mater.** 2015; 27, 4296–4301. Doi: 10. 1002/adma. 201501708

[16] van Manen T, Janbaz S, Ganjian G, and Zadpoor AA. Kirigami-enabled self-folding origami. **Materials Today** 2020; 32, 59-67. Doi: 10. 1016/j. mattod. 2019. 08. 001

[17] Meng Z, Chen W, Mei T, Lai Y, Li Y, and Chen CQ. Bistability-based foldable origami mechanical logic gates. **Extreme Mechanics Letters** 2021; 43, 101180. Doi: 10. 1016/j. eml. 2021. 101180

[18] Wang C, Huang Z, Chen Z, and Li Y. A novel polar mechanical metamaterial with dual deformation characteristics. **International Journal of Mechanical Sciences** 2024; 264. Doi: 10. 1016/j. ijmecsci. 2023. 108827

[19] Yang Q, Li Z, Hao H, and Chen W. Compressive mechanical properties and dynamic behaviour of origami-inspired tri-directional auxetic metastructure. **Engineering Structures** 2023; 281. Doi: 10. 1016/j. engstruct. 2023. 115751

[20] Sun X, Wu S, Dai J, Leanza S, Yue L, Yu L, Jin Y, Qi HJ, and Zhao RR. Phase diagram and mechanics of snap-folding of ring origami by twisting. **International Journal of Solids and Structures** 2022; 248. Doi: 10. 1016/j. ijsolstr. 2022. 111685

[21] Meng Z, Qin W, Mei T, and Chen CQ. Bi-material sinusoidal beam-based temperature responsive multistable metamaterials. **International Journal of Solids and Structures** 2023; 277-278. Doi: 10. 1016/j. ijsolstr. 2023. 112343

[22] Liu N, Becton M, Zhang L, Tang K, and Wang X. Mechanical anisotropy of two-dimensional metamaterials: a computational study. **Nanoscale Advances** 2019; 1, 2891. Doi: 10. 1039/c9na00312f

[23] Kabir S, Kim H, and Lee S. Characterization of 3D Printed Auxetic Sinusoidal Patterns/Nylon Composite Fabrics. **Fibers and Polymers** 2020; 21(6), 1372-81. Doi: 10. 1007/s12221-020-9507-6

[24] Li P, Zhang X, Zhang Z, and Wen Q. Application of Re-Entrant Honeycomb Auxetic Structure in Force Measurements. **IEEE Sensors Journal** 2021; 21. Doi: 10. 1109/JSEN. 2021. 3102960

[25] Gibson LJ, Ashbay MF, Schajer GS, and Robertson CI. The mechanics of two-dimensional cellular materials. **Proc. R. Soc. Lond. A** 1982; 382:25